Design and Computational Flow Analysis of Different Rocket Nozzle Profile

Bhupendra Kumar[1], Mohd Shoaib[2], Ramanan G[3] & Radhakrishnan P [4]

[1,2] Student, [3,4]Faculty, Department of Aeronautical Engineering

ACS College of Engineering, Bengaluru

***DOI**: https://doi.org/10.34293/acsjse.v2i2.38*

Abstract - *In recent days the launching value of increasing the industrial business starts with lowering prices related to the launch vehicle operation. Reducing the price begins with rising the propulsion systems, creating these vehicles a lot of economical with a restricted fuel amount. The Linear Aerospike engine has incontestable bigger thrust potency over this engines used on launch vehicles. However, unresolved problems with warming plague this standard. This study proposes an approach amendment to the rocket motor that explores a way to increase the performance of the nozzle body, and lower the chance of failure because of the acute pressure environments. The results show that however the most exhaust flow of an Aerospike is full of couture of the spike surface. Victimization in Ansys CFD software system and acting a straight forward experiment with whoosh rockets, the study explores however exhaust flow changes the performance characteristics, in the main speed close to the wall. The results with some improvement is created by CFD nozzle flow studies, to make sure the bottom pure mathematics isn't a contributory issue to the film-cooling results.*

Keywords: *Nozzle, launch vehicle, Rockets. CFD*

I INTRODUCTION

Nozzles are used in rocket engines to expand and accelerate the combustion gases, from burning. When the fluid flows through the nozzle it exits at a higher velocity than its inlet velocity. The de Laval nozzle is used to increase the velocity of exhaust plumes at the exit of the nozzle at supersonic speed where the pressure is ideally equal to or more than that of atmospheric pressure for efficient flow of exhaust gases and increase the thrust. The combustion products are allowed to expand with an exit velocity resulting in the thrust of the engine. From the authors it is found that the aerospike nozzle may be a bell nozzle with its nozzle profile turned within out. Flow of combustion gases is directed radially inward towards the nozzle axis. Ahmed Mahjub et al. studied that solid rocket motors (SRMs) established to be a reliable and cost- effective system thanks to their easy manufacture, long-lifetime storage along side the short time required for launching, and an excellent deal of chemical mechanical energy. Yamanishi et al. bestowed to develop a next generation booster engine named LE-X that may be a successor of LE-7A. Author additionally studied regarding multi-objective style optimisation with generic formula was applied to the rotary engine blade form.

The optimized results show robust exchange between axial-horsepower and entropy-rise among the stage. Desikan et al conducted experiments on a blunt-cone-cylinder pure mathematics with numerous increasing aft body configurations and bestowed the results of the result free stream (M= 5)-jet plume (M= two.65) interaction on mechanics coefficients. Taro Shimizu et al studied flow structures within and outdoors a rocket nozzle, that ar indispensable for actual development of rocket and numerically reproduced beneath the process wherever the transition happens. Ankit Kumar et al. designed the Solid Rocket case and the nozzle of the Solid Rocket Motor using Solid Works software. The designs have been developed to achieve a high thrust vector. Novi Andria et al exposed to extreme temperature and pressure resulted from gas combustion and found that the nozzle must be able to maintain structural integrity when exposed to such environment. From the literature study in this work using Ansys CFD software system a straight forward experiment with rockets nozzles will be conducted and the study will explores however exhaust flow changes the performance characteristics, in the main speed close to the wall.

II DESIGN METHODOLOGY

For designing the nozzle contour the most significant step, that varies in keeping with the operational conditions and purpose. Conversely, the look procedure, as well as the essential theory after the C-D nozzle style remains an equivalent. The look will be done employing a straightforward estimated methodology or Rao's methodology supported various calculations.

$$\frac{A_{exit}}{A^*} = \left[\frac{1}{M_{exit}}\left[\left(\frac{2}{\gamma+1}\right)\left(1+\frac{(\gamma-1)}{2}M_{exit}^{\ 2}\right)\right]^{\frac{\gamma+1}{2(\gamma-1)}}\right] =$$

$$\frac{1}{M_{exit}}\sqrt{\left[\left[\left(\frac{2}{\gamma+1}\right)\left(1+\frac{(\gamma-1)}{2}M_{exit}^{\ 2}\right)\right]^{\frac{\gamma+1}{(\gamma-1)}}\right]}$$

In this study the methodology predicts a series of targeted physical property which cowl lip of the spike nozzle enlargement waves occurring inside. By preferring this methodology, the ringed spike contour for a specified pressure quantitative relation, space at throat, and quantitative relation of specific heats is estimated. The enlargement quantitative relation is decided for the consequent pressure quantitative relation from the relation that specifies the difference between the exit pressures. The formula to calculate best nozzle throat space is;

Table 1 Input for CEA analysis of Propanol

Altitude (km)	Pressure (atm)	Oxygen/Fuel ratio	Area ratio (Ae/At)	Temperature (K)
0	1.01325	2.4	1.80314	888.285
5	0.540733	1.8	2.76551	814.918
10	0.265035	1.2	4.64164	727.542
15	0.121113	0.6	8.4354	627.756

Table 2 Input for CEA analysis of Ethanol

Altitude (km)	Pressure (atm)	Oxygen/Fuel ratio	Area ratio (Ae/At)	Temperature (K)
0	1.01325	2	1.80551	874.522
5	0.540733	1.5	2.76642	802.804
10	0.265035	1	4.64021	718.633
15	0.121113	0.5	8.42388	623.978

2.1 CFD ANALYSIS

By considering the flow cold to calculate, the values of chamber temperature (Ti=300K), heat Ratio (γ=1.13) and R of exhaust (R=287) are considered as the perfect gas. For each style there needs to be at least a parameter are going to be thought-about constant to see the opposite style parameter standards. At this point, for the aerospike nozzle style, Nozzle Pressure quantitative relation (NPR=20) and Mass rate (2Kg/S) were considered as constant. The different basic parameters supported the worth of mass rate and perfect gas constant values were determined by second physical property Flow Equations. These inputs are taken from CEA analysis result.

Conical C – D nozzle

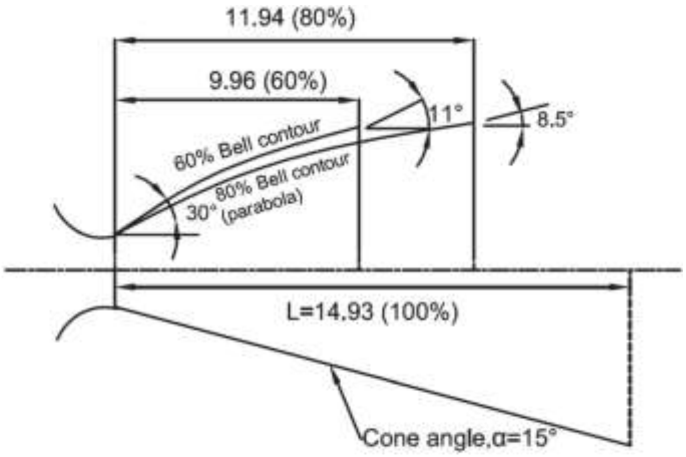

Figure 1 Rao's method based on calculus of variation

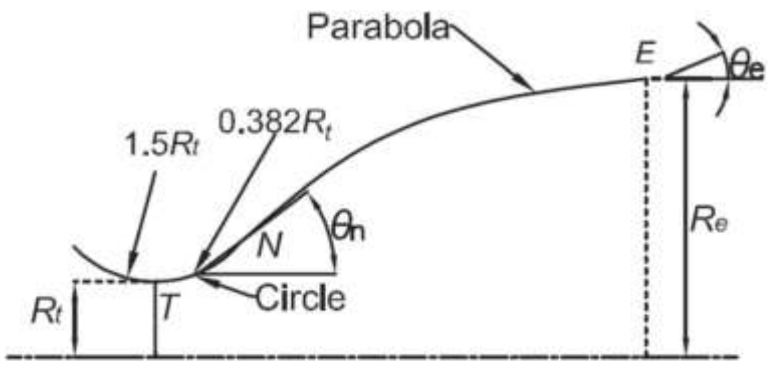

Figure 2 Parabolic approximation bell nozzle design configuration

2.2 Design Aspects Of Nozzle

Conical Nozzle

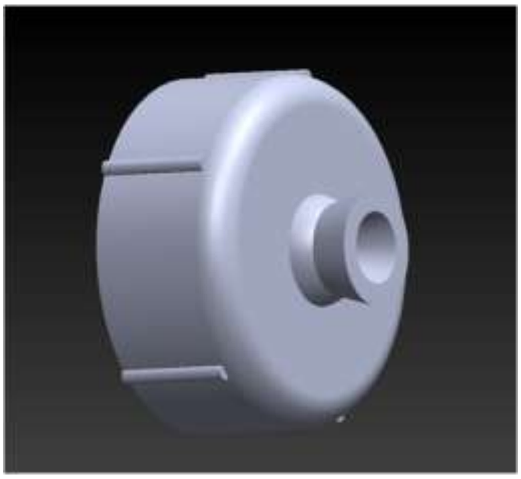

Fig.1a Isometric View

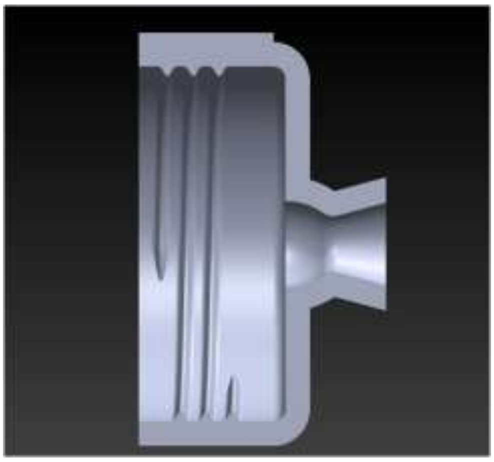

Fig 1b Side View

Bell Nozzle

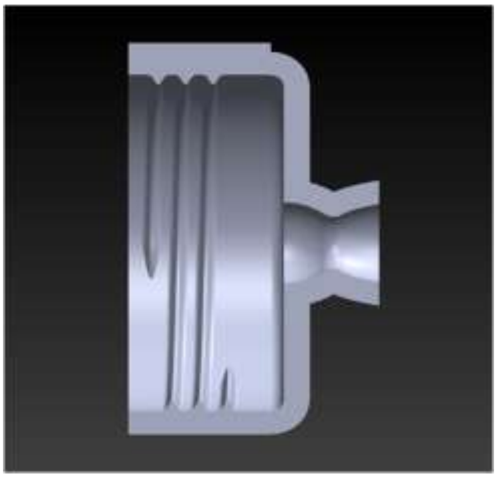

Fig 2a Side View

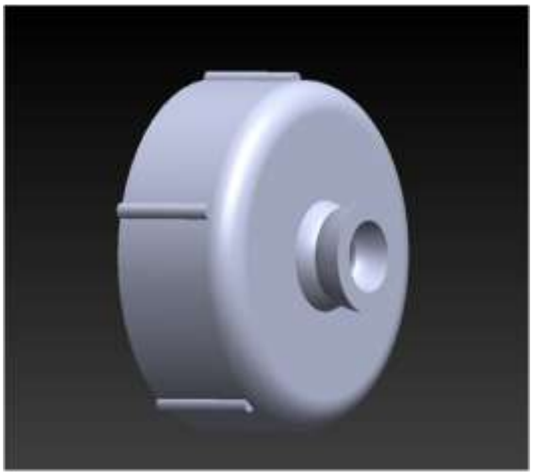

Fig 2b Isometric view

Aerospike 60º cone Nozzle

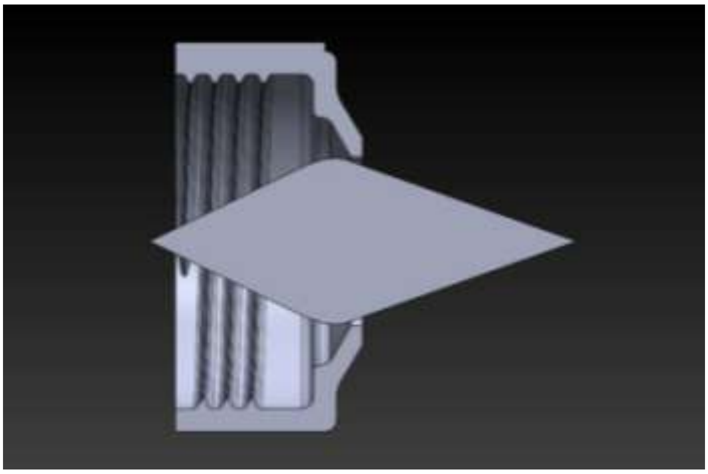

Fig 3a Side View

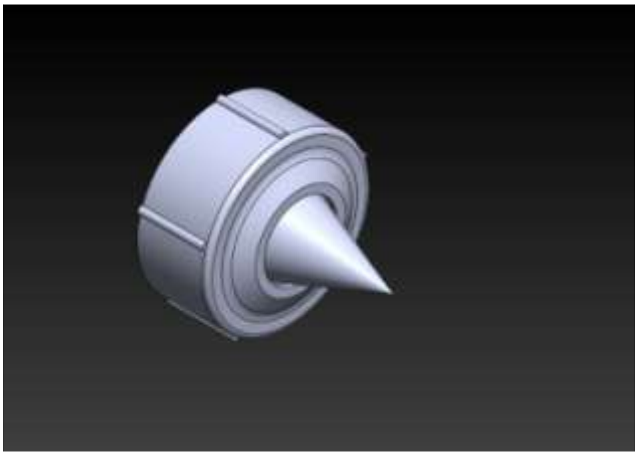

Fig 3b Isometric view

Aerospike circular cone Nozzle

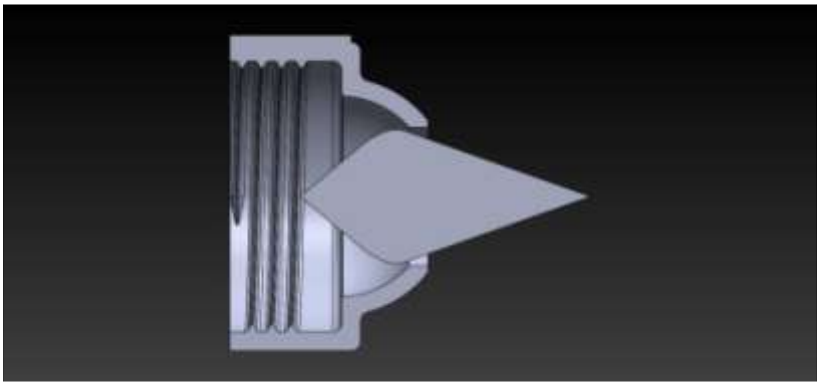

Fig 4a Side View

Fig 4b Isometric view

Optimized 60º Aerospike Nozzle

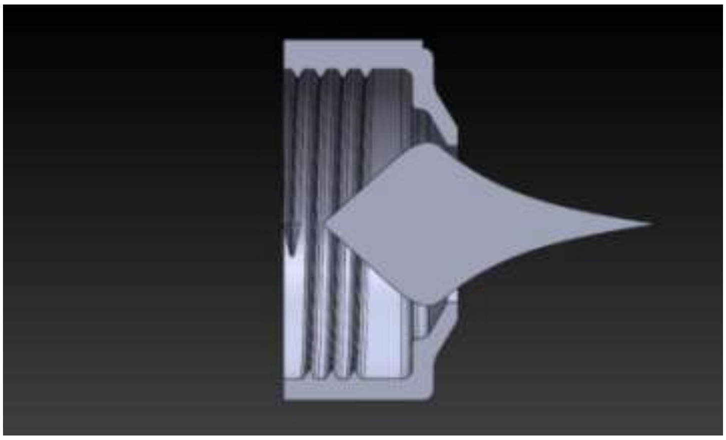

Fig 5a Side View

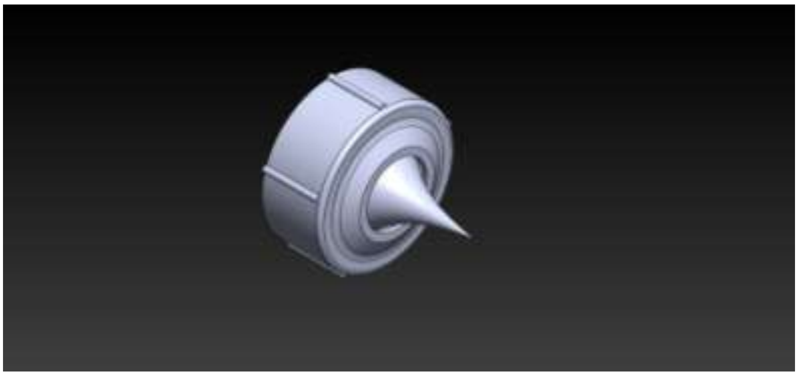

Fig 5b Isometric view

Optimized circular Aerospike Nozzle

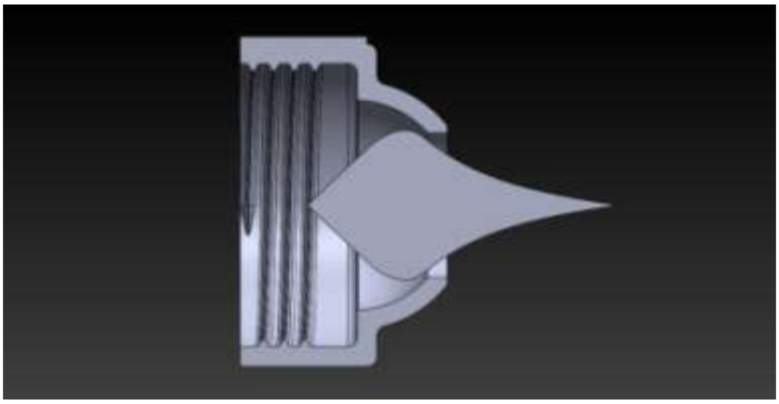

Fig 6a Side View

Fig 6b Isometric view

III EXPERIMENTATION & ANALYSIS

In this work the nozzle design is so obtained to simulate optimization procedure fluid dynamics package ANSYS FLUENT version 12.01 and therefore the post process of the results, for the primary style reveals the issues within the style and so the look is changed. The images below show the recent style, its CFD analysis and therefore the new style. Several new styles is simulated through the package associated an optimized curve is obtained so giving the very best potency nozzle style. during this work we've used the woosh rocket bottle for experiment wherever we have a tendency to used alcohol and grain alcohol as fuel and optimized the nozzle supported the scale if bottle cap. Fig.1 to Fig.6 shows the isometric and vista of style aspects of nozzle.

Table 3 Experiment results

Altitude (km)	Parameters	Inlet	Outlet	Far field
0	Pressure (atm)	5.6	1	1
	Temperature (K)	1035	298	298
5	Pressure (atm)	5.6	0.53	0.53
	Temperature (K)	1035	298	298

3 Results and Discussion

Table 4 Table of input parameters

Atmospheric Pressure (atm)	Nozzle Type	Exit Velocity (mach)	Exit Pressure (atm)
1	Conical	1.87	1.36
	Bell	1.94	1.22

Table 5 Optimized Aerospike Value

Atmospheric Pressure (atm)	Nozzle Type	Exit Velocity (mach)	Exit Pressure (atm)
1	Aerospike 60º angled	1.92	1.36
	Aerospike circular	2	1.22
0.53	Aerospike 60º angled	2.27	1.09
	Aerospike circular	2.15	0.81

4.1 Velocity Contour results

Conical Nozzle at Sea level

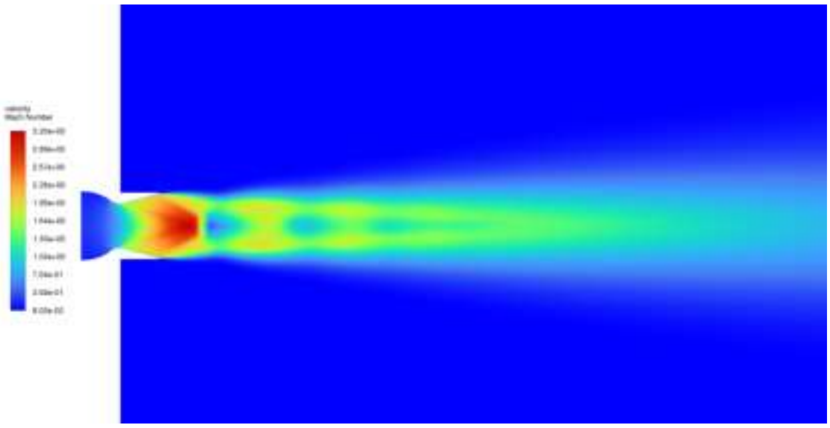

Analysis of Conical Nozzle 5km Above Sea level

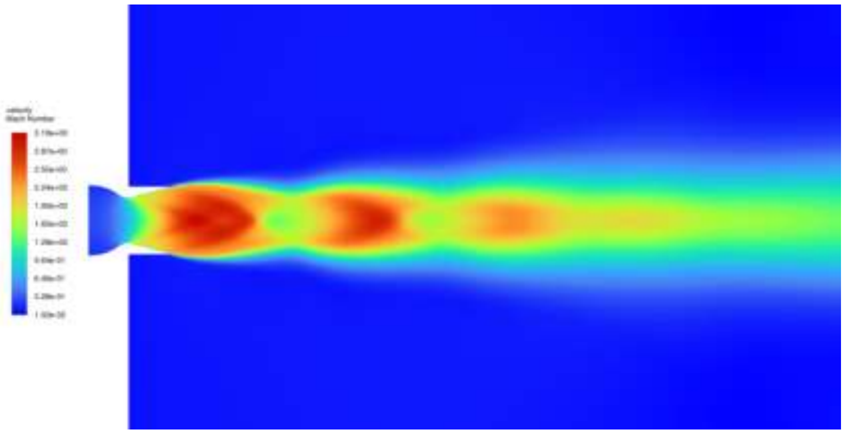

Bell Nozzle at Sea level

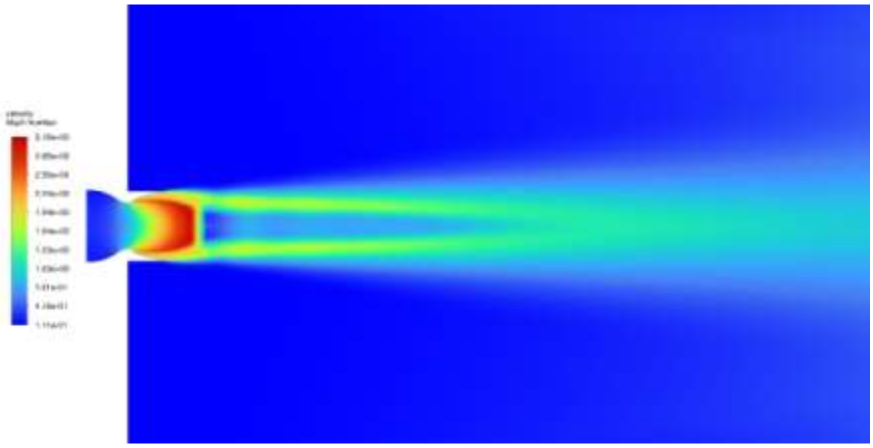

CFD Analysis of Bell Nozzle 5km above Sea level

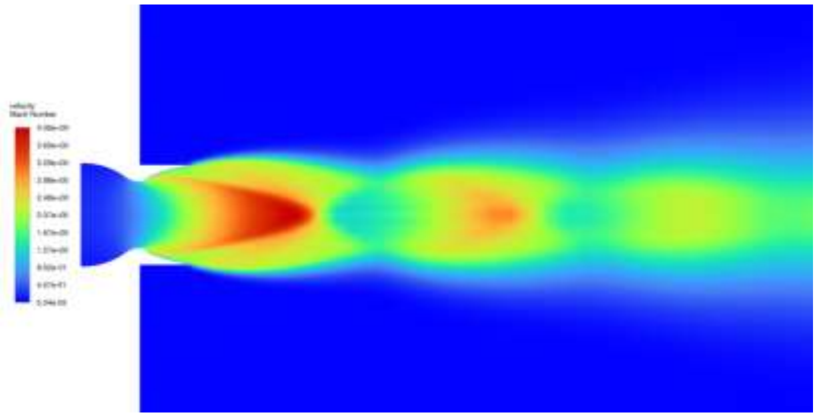

Aerospike cone 60°angled at Sea level

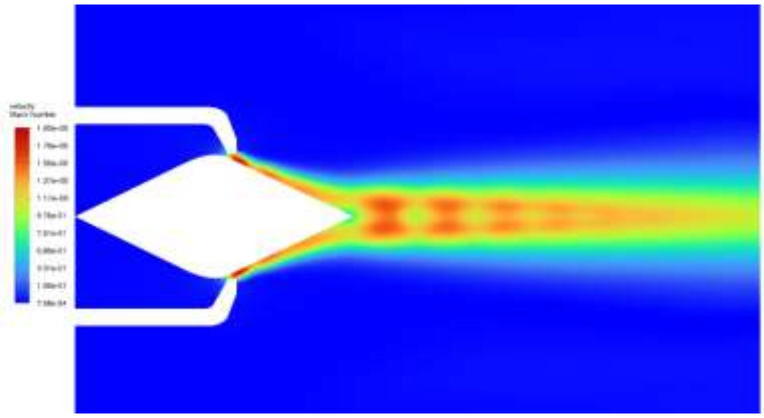

Aerospike cone 60°angled above 5km Sea level

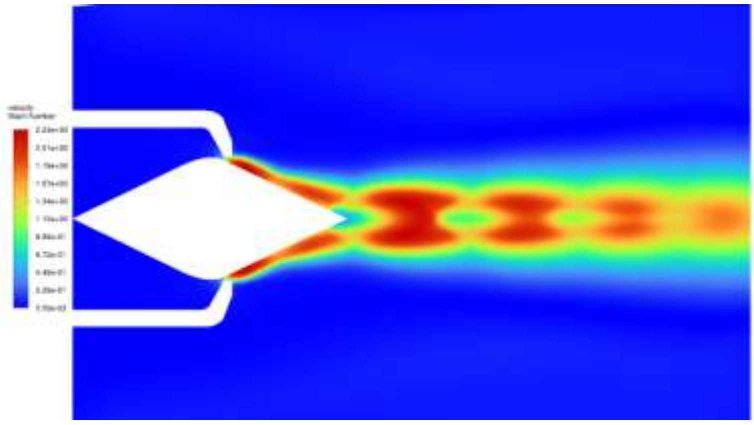

Optimized Aerospike 60 º angled Nozzle at Sea level

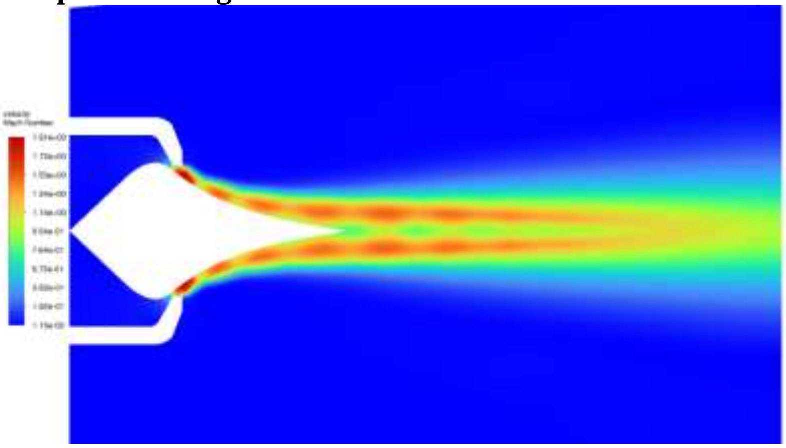

Optimized Aerospike 60 º angled 5km above Sea level

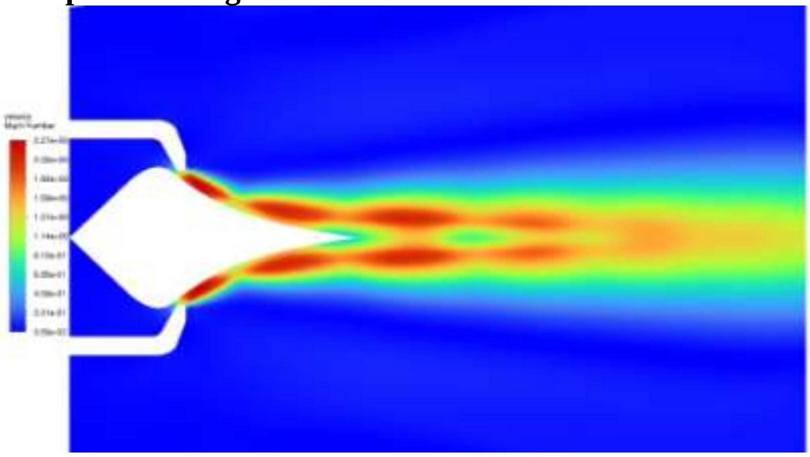

Optimized Aerospike circular at Sea level

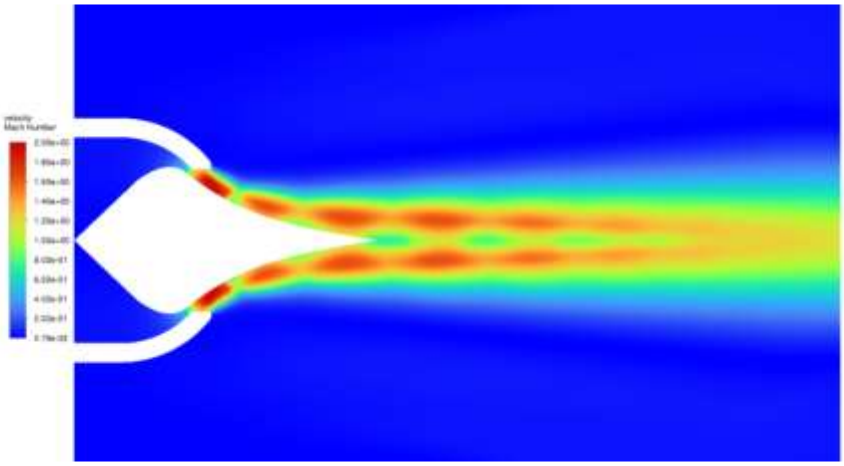

Optimized Aerospike circular 5 km above Sea level

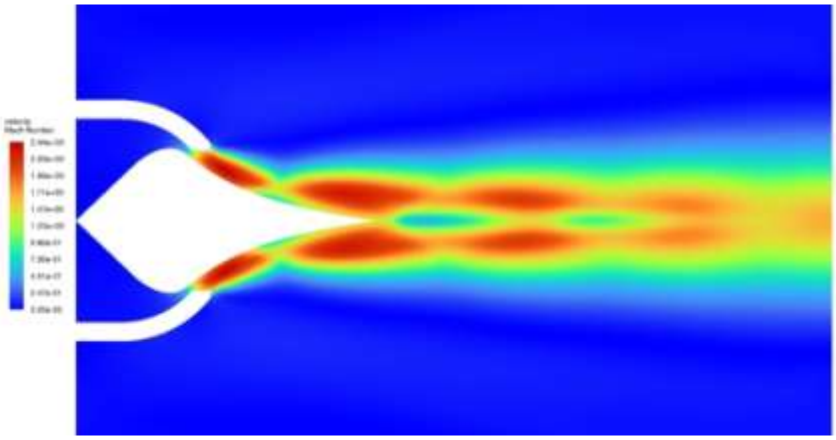

V CONCLUSION

The flow characteristics and numerous performance indicators are analysed to see the result of various the nozzle at close to optimum and over-expansion conditions. The speed contours clearly demonstrate the result the varied conditions wear the exhaust flow, because the recirculating flow region can become larger in over-expansion conditions associate degreed manufacturing an open wake. as compared a closed wake is created at close to optimum conditions. As a result, the negative thrust contribution of the bottom will increase with relation to optimum conditions. This result is accentuated once the pressure at the water is increased. At close to optimum conditions, all aerospike nozzles demonstrate a performance gain over the bell nozzle. this is often because of the fast decline within the bell nozzles potency at low altitudes, differing from the aerospike nozzle. this is often highlighted by a bigger performance of the aerospike nozzle at a lower NPR.

REFERENCES

[1] Petrova, T., & Petrov, Z. (2020). Analysis on the Leading Trends and Capabilities of UAV 'S and Their Application in the European Cooperation Projects. International E-Journal of Advances in Social Sciences, 6(16), 137-144.

[2] Merino, L., Caballero, F., Martínez-de Dios, J. R., Ferruz, J., & Ollero, A. (2006). A cooperative perception system for multiple UAVs: Application to automatic detection of forest fires. Journal of Field Robotics, 23(3-4), 165-184.

[3] Sri, K. R. B., Aneesh, P., Bhanu, K., & Natarajan, M. (2016). Design analysis of solar-powered unmanned aerial vehicle. Journal of Aerospace Technology and Management, 8, 397-407.

[4] André, N. O. T. H. (2008). Design of solar powered airplanes for continuous flight. DISS ETH, 18010.

[5] VS, B., Petruchik, V. P., & Kuznetsov, A. V. (2013). Investigation of wing airfoils for low-speed high-altitude unmanned aerial vehicles. Aircraft Engineering, 20(3), 19-31.

[6] Jashnani, S., Nada, T. R., Ishfaq, M., Khamker, A., & Shaholia, P. (2013). Sizing and preliminary hardware testing of solar powered UAV. The Egyptian Journal of Remote Sensing and Space Science, 16(2), 189-198.

[7] Oettershagen, P., Melzer, A., Mantel, T., Rudin, K., Stastny, T., Wawrzacz, B., & Siegwart, R. (2017). Design of small hand-launched solar-powered UAVs: From concept study to a multi-day world endurance record flight. Journal of Field Robotics, 34(7), 1352-1377.

[8] Panagiotou, P., Kaparos, P., & Yakinthos, K. (2014). Winglet design and optimization for a MALE UAV using CFD. Aerospace Science and Technology, 39, 190-205.

[9] Gryte, K., Hann, R., Alam, M., Roháč, J., Johansen, T. A., & Fossen, T. I. (2018, June). Aerodynamic modeling of the skywalker x8 fixed-wing unmanned aerial vehicle. In 2018 International Conference on Unmanned Aircraft Systems (ICUAS) (pp. 826-835). IEEE.

[10] Lee, B., Park, P., Kim, K., & Kwon, S. (2014). The flight test and power simulations of an UAV powered by solar cells, a fuel cell and batteries. Journal of Mechanical Science and Technology, 28(1), 399-405.

[11] Fan, B., Li, Y., Zhang, R., & Fu, Q. (2020). Review on the technological development and application of UAV systems. Chinese Journal of Electronics, 29(2), 199-207.

[12] Suzuki, K. A., Kemper Filho, P., & Morrison, J. R. (2012). Automatic battery replacement system for UAVs: Analysis and design. Journal of Intelligent & Robotic Systems, 65(1), 563-586.

[13] Klippstein, H., Hassanin, H., Diaz De Cerio Sanchez, A., Zweiri, Y., & Seneviratne, L. (2018). Additive manufacturing of porous structures for unmanned aerial vehicles applications. Advanced Engineering Materials, 20(9), 1800290.

[14] Chu, Y., Ho, C., Lee, Y., & Li, B. (2021). Development of a solar-powered unmanned aerial vehicle for extended flight endurance. Drones, 5(2), 44.